

**Evaluation of mesostructured silicas with wormhole-like framework functionalized with hydrophobic groups as alternative sorbents for extraction of drug residues from food samples**

**Natalia Casado, Sonia Morante-Zarcero, Damián Pérez-Quintanilla, Isabel Sierra\***

Departamento de Tecnología Química y Energética, Tecnología Química y Ambiental, Tecnología Mecánica y Química Analítica, E.S.C.E.T, Universidad Rey Juan Carlos, C/ Tulipán s/n, 28933 Móstoles, Madrid, Spain

\* Corresponding author: Tel.: (+34) 914887018; fax: (+34) 914888143.

*E-mail address:* [isabel.sierra@urjc.es](mailto:isabel.sierra@urjc.es)

## ABSTRACT

---

Different mesostructured silicas were synthesized and functionalized with octadecylsilane groups under same conditions. All materials were characterized and evaluated as sorbents for simultaneous multi-residue extraction of veterinary drugs from bovine meat samples by solid-phase extraction prior to their chromatographic analysis coupled to tandem mass spectrometry. The results obtained were compared to select the material with the highest extraction potential to achieve this purpose.

**Keywords** Functionalized mesostructured silicas, SPE, Veterinary drugs, Hydrophobic functional groups

## 1. Introduction

One of the main concerns of the food field is to monitor the presence of veterinary drug residues in food products, because the long-term exposure to these substances constitutes a potential health risk for consumers since it can induce different toxic, carcinogenic and teratogenic side effects [1]. Generally, a sample preparation method is often required prior to further analysis of these substances, being solid phase extraction (SPE) the most widely used to isolate and purify residual veterinary drugs from meat solvent extracts [2].

Recent advances in the development of mesostructured silicas have promoted their application as SPE sorbents. Nevertheless, only a few studies use them as sorbents for extraction and pre-concentration of organic contaminants from food matrices [3]. In this sense, mesoporous silicas with hexagonal ordered pore structure, SBA-15 and MCM-41, functionalized with different organic ligands, have been the main mesostructured silicas applied for the extraction of organic contaminants from food matrices [3], but to best of our knowledge, other families of mesostructured silicas with wormhole-like frameworks, such as HMS and MSU-2, have never been evaluated with this purpose.

The aim of this study was to evaluate for the first time the application of different silicas with wormhole-like pore arrangement as SPE sorbents, in order to select the most suitable for the multi-residue extraction of 26 residual veterinary drugs from meat samples prior to their chromatographic determination. Additionally, two hybrid mesoporous silicas with ordered hexagonal pore arrangement were synthesized for comparison purposes.

## 2. Experimental

### 2.1. Synthesis of mesostructured silicas

HMS [4], MSU-2 [5], ethane-PMO [6], SBA-15 [7] and MCM-41 [8], were prepared according to previous works.

HMS mesoporous silica was synthesized following the method described by Pérez-Quintanilla et al. [4] with slight modifications. 30 g of DDA were dissolved in 388.8 mL of Milli-Q water and 227.4 mL of ethanol. The solution was stirred until its homogenization, and subsequently 124.8 g of TEOS were added drop by drop. The solution was stirred for 18 h, yielding a thick white suspension that was filtered and dried at 80 °C for 1 h. The amine was removed by heating the solid at reflux in ethanol with a Soxhlet for 8 h. Finally, the rest of surfactant was removed by calcination at 550 °C for 18 h.

MSU-2 mesoporous silica was prepared according to Pérez-Quintanilla et al. [5]. 78.2 g of Tergitol® NP-9 were mixed with 1562 mL of Milli-Q water. The solution was stirred at room

temperature, and once it was homogenous, 52.82 g of TEOS were added drop by drop. The resulting suspension was then aged without stirring for 20 h. After this time, 26.4 mL of 0.24 M sodium fluoride solution were added dropwise with stirring. The resultant solution was then placed in a bath with stirring at 55 °C for 48 h. The final product was filtered, washed with Milli-Q water and dried at 100 °C for 4 h. Finally, the surfactant was removed by calcination at 600 °C for 12 h.

Ethylene-bridged organosilica (denoted as ethane-PMO) was prepared according to the method described by Zhu et al. [6]. Briefly, 8.85 g of Pluronic 123 and 1.53 g of CTAB, were dissolved in a solution formed by 101.1 mL of HCl 2 M, 92.09 mL of ethanol and 741.17 mL of Milli-Q water, the mixture was stirred for 30 minutes. After this time 7.51 g of BTME were added drop by drop, the solution was transferred into a Teflon-lined steel Parr autoclave and heated at 100 °C during 16 h. The white precipitate was recovered by filtration, washed with Milli-Q water and the surfactant was extracted in Soxhlet with a mixture of ethanol and HCl (97:3, v/v) for 24 hours.

SBA-15 mesoporous silica was prepared as follows: 48.4 g of Pluronic 123 were dissolved in 1440 g of 2 M HCl solution and 360 mL of Milli-Q water with stirring at 35 °C. Then, 102 g of TEOS were slowly added, and the resulting mixture was stirred at the same temperature for 20 h. After this reaction time, the stirring was stopped and the temperature was increased to 80 °C and maintained for 24 h. The solid product was recovered by filtration and washed with water. Then, it was calcined at 500 °C for 18 h [7].

MCM-41 mesoporous silica was prepared according to Landau et al. [8] using hydrothermal crystallization with slight modifications. 65.45 g of sodium silicate solution were mixed with 2.28 mL of 98% sulfuric acid and 140 mL of Milli-Q water. The mixture was stirred for 30 min at room temperature. Afterwards, 58.66 g of CTAB dissolved in 176 mL of Milli-Q water were added. The resulting gel was mixed with 70 mL of Milli-Q water and stirred at room temperature for 30 min. The gel was transferred to a Teflon-coated autoclave and heated at 121 °C for 144 h. The resultant solid was separated by filtration and dried at 100 °C for 8 h. The surfactant was removed by calcination at 530 °C for 18 h.

## *2.2. Modification of mesostructured silicas with C18 groups*

The obtained materials were modified with chloro(dimethyl)octadecylsilane (C18) under same conditions. For this purpose, 8 g of each mesostructured silica (HMS, MSU-2, ethane-PMO, SBA-15 and MCM-41) were mixed with 50 mL of toluene and 1.2 g of C18. The mixture was heated at 80 °C for 24 h at 500 rpm. The resultant materials (denoted as HMS-C18, MSU-2-C18, ethane-PMO-C18, SBA-15-C18 and MCM-41-C18) were recovered by filtration and washed with two fractions of 50 mL of toluene, ethanol and diethyl ether.

### *2.3. Characterization of mesostructured silicas*

All materials were characterized by transmission electron microscopy (TEM), scanning electron microscopy (SEM), nitrogen adsorption-desorption isotherms, elemental analysis and thermogravimetric analysis (TGA).

SEM and morphological analysis were carried out on a XL30 ESEM Philips with an energy-dispersive spectrometry system (EDS). The samples were treated with a sputtering method with the following parameters: sputter time 100 s, sputter current 30 mA, and film thickness 20 nm using sputter coater BAL-TEC SCD 005. TEM was performed on a TECNAI 20 Philips microscope operating at 200 kV, with a resolution of 0.27 nm and  $\pm 70^\circ$  of sample inclination, using a BeO sample holder. Nitrogen gas adsorption-desorption isotherms were performed using a Micromeritics ASAP 2020 analyzer. Elemental analysis (% H, % C and % N) were performed using a microanalyser model LECO CHNS-932. The thermal stability was studied using a Setsys 18 A (Setaram) thermogravimetric analyzer with a 100  $\mu$ L platinum crucible. A synthetic air atmosphere was used and the temperature increased from 25  $^\circ$ C to 800  $^\circ$ C at a speed of 10  $^\circ$ C per minute.

### *2.4. Extraction procedure and chromatographic analysis*

2 g of spiked minced meat were mixed with 10 mL of acetate buffer 0.2 M (pH 5.2), vortexed 1 min and centrifuged at 3500 rpm for 10 min. The supernatant was collected, and the residue re-extracted with 5 mL of acetate buffer 0.2 M (pH 5.2) and 5 mL of MeOH, vortexed 1 min and centrifuged at 5000 rpm for 10 min. The resultant supernatant was collected with the previous one, filtered under vacuum and purified by SPE. SPE cartridges were packed with 100 mg of mesostructured silica and plugged with polyethylene frits at both ends, also a 0.45  $\mu$ m nylon filter membrane was inserted at the bottom to prevent material loss during sample loading. Cartridges were initially conditioned with 2x2 mL MeOH and 2x2 mL Milli-Q water at a flow rate of 1 mL min<sup>-1</sup>. After sample extract loading, cartridges were dried, and afterwards washed with 1x5 mL Milli-Q water to remove interferences. Elution was performed with 2x2 mL MeOH. The eluate was evaporated to dryness and re-dissolved with 500  $\mu$ L of MeOH for subsequent analysis in the chromatographic system.

Chromatographic separation was performed on an UHPLC system (Dionex UltiMate 3000, Thermo Scientific, MA, USA) coupled to an ion trap mass spectrometer detector (Bruker) using an ACE Excel 2 C18 column (100 mm x 2.1 mm, 2  $\mu$ m particle size, ACE, UK) at 30  $^\circ$ C, the injection volume was 10  $\mu$ L and the flow rate was 0.3 mL min<sup>-1</sup>. A binary mobile phase was used, combining: ACN (phase A) and water (phase B), both containing 0.1% formic acid and 4 mM ammonium acetate, with a initial composition of 20% A and 80% B. For gradient elution, phase A increased linearly to 100% in first 6 min, and then returned to initial conditions in 2 min. The column was then equilibrated for 2 min prior to next injection, yielding a total run-time analysis of 10 min. Mass spectrometry acquisition was

carried out using electrospray ionization interface (ESI) operating in both positive and negative ion mode, and multiple reaction monitoring (MRM) mode was used for all analytes. Capillary voltage was held at -4500 V and the end plate offset at -500 V. The nebulizer was set at 20 psi, the dry gas at 10 L min<sup>-1</sup>, and the dry temperature at 200 °C. Supporting information Table 1 summarizes retention time, ionization mode, fragmentation amplitude and product ions (daughter and granddaughter ions) selected for each analyte during MRM acquisition.

**Table 1** Mass spectrum parameters, retention time and spiking level for the target analytes using UHPLC-IT-MS/MS

Analyte	Spiked level ( $\mu\text{g Kg}^{-1}$ )	Ionization mode	Retention time (min)	Precursor ion ( $m/z$ )	Fragmentation amplitude	MS <sup>2</sup> . Daughter ions <sup>1</sup> ( $m/z$ )	Fragmentation amplitude	MS <sup>3</sup> . Granddaughter ions ( $m/z$ )
Cimaterol	5 <sup>a</sup>	ESI (+)	1.4	220	0.60	202*, 160		
Terbutaline	10 <sup>b</sup>	ESI (+)	1.4	226	0.70	170, 152*		
Salbutamol	5 <sup>b</sup>	ESI (+)	1.4	240	0.60	222*, 166		
Atenolol	5 <sup>a</sup>	ESI (+)	1.4	267	0.50	225, 190*		
Ractopamine	10 <sup>c</sup>	ESI (+)	1.6	302	0.50	284*, 164		
Clenproperol	5 <sup>a</sup>	ESI (+)	1.8	263	0.70	245*, 203		
Acebutolol	5 <sup>a</sup>	ESI (+)	1.8	337	0.60	319*, 260		
Metoprolol	5 <sup>a</sup>	ESI (+)	2.1	268	0.60	191*, 116		
Tulobuterol	0.2 <sup>a</sup>	ESI (+)	2.1	228	0.70	172, 154*		
Clenbuterol	0.2 <sup>c</sup>	ESI (+)	2.2	277	0.60	259*, 203		
Brombuterol	5 <sup>a</sup>	ESI (+)	2.6	367	0.70	349*, 293		
Carazolol	5 <sup>c</sup>	ESI (+)	2.9	299	0.70	222*, 116		
Labetalol	5 <sup>a</sup>	ESI (+)	2.9	329	0.50	311*, 207		
Mabuterol	5 <sup>a</sup>	ESI (+)	2.9	311	0.70	293*, 237		
Propranolol	5 <sup>a</sup>	ESI (+)	3.4	260	0.50	183*, 116		
Betaxolol	5 <sup>a</sup>	ESI (+)	3.5	308	0.70	177, 116*		
$\alpha$ -Zearalanol	2 <sup>c</sup>	ESI (-)	4.3	321	0.70	303, 277*		
Ketoprofen	5 <sup>a</sup>	ESI (+)	4.9	255	0.50	209*	0.70	194, 131, 105
Naproxen	10 <sup>b</sup>	ESI (+)	4.9	231	0.80	185*	0.70	170
Meloxicam	20 <sup>c</sup>	ESI (+)	4.9	352	0.60	141, 115*		
Flunixin	20 <sup>c</sup>	ESI (+)	5.2	297	0.70	279*, 257		
Carprofen	50 <sup>a</sup>	ESI (-)	5.6	272	0.60	228*	0.40	226
Diclofenac	5 <sup>c</sup>	ESI (-)	5.8	294	0.70	250*	0.70	214, 178
Ibuprofen	100 <sup>a</sup>	ESI (-)	6.1	205	1.00	161*, 159		
Tolfenamic acid	50 <sup>c</sup>	ESI (-)	6.7	260	0.50	216*	0.60	180
Vedaprofen	50 <sup>c</sup>	ESI (+)	7.3	300	1.00	201, 155*		

<sup>1</sup> Predominant product ions. \* Ions used for quantitation. Isolation width ( $m/z$ ) is 4. <sup>a</sup> Specific level of interest based on the drug characteristics and its detection in the ion trap mass spectrometer and in the analytical method. <sup>b</sup> Recommended concentration (EURL requirements) [18]. <sup>c</sup> Maximum Residue limit (MRL) [18]. Chromatographic conditions: t = 0 min, 20 % A – 80 % B, t = 6 min, 100 % A, t = 8 min, 20 % A – 80 % B (2 min) (ACN as mobile phase A and water as mobile phase B, both containing 0.1 % formic acid and 4 mM ammonium acetate). The flow rate was 0.3 mL min<sup>-1</sup>.

### 3. Results and discussion

#### 3.1. *Mesostructured silicas characterization*

Nitrogen adsorption-desorption isotherms of the materials are shown in Fig. 1a. HMS, MSU-2, ethane-PMO, SBA-15 and MCM-41 isotherms were type IV according to IUPAC classification with a narrow hysteresis loop representative of mesoporous solids. SBA-15 showed a H1 hysteresis loop, indicative of uniform cylindrical pores; MSU-2 and MCM-41 almost showed no hysteresis loop because their pore sizes fall in the range of small mesopores; while HMS and ethane-PMO showed a H2 hysteresis loop, indicative of wormhole-like pores causing some bottleneck effect. Pore size distribution of the materials was calculated using Barrett-Joyner-Halenda method, obtaining narrow pore size distributions for SBA-15, MCM-41 and MSU-2 (Fig. 1b), which provided evidence for uniform framework mesoporosity. Conversely, in HMS and ethane-PMO, the capillary condensation/evaporation step was not very sharp, therefore their pore sizes were not too uniform, showing more than one maximum (Fig. 1b).

MCM-41 showed the highest surface area ( $S_{\text{BET}}$ ), but small pore diameter (1101  $\text{m}^2/\text{g}$  and 30 Å, respectively), while SBA-15 showed the lowest  $S_{\text{BET}}$  and the highest pore diameter (764  $\text{m}^2/\text{g}$  and 65 Å, respectively) (Table 2). Surface modification with C18 left the overall appearance of these isotherms practically unchanged (Fig. 1a), however, after functionalization the  $S_{\text{BET}}$  and pore volume decreased (Table 2), together with slight reductions in pore diameter (Fig. 1b), what can be attributed to the presence of C18 groups which, due their big size, were mainly grafted on the external surface of the materials.



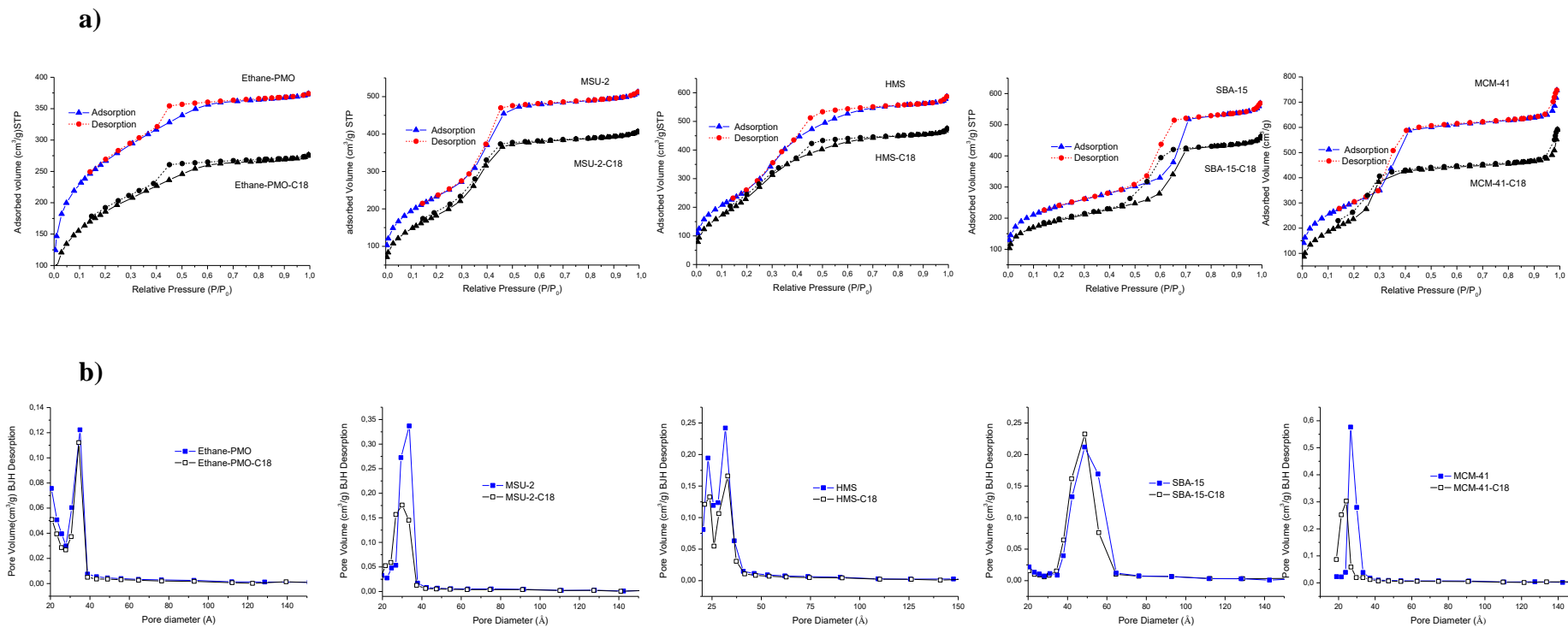


**Fig. 1** (a)  $N_2$  adsorption-desorption isotherms and (b) pore size distribution of synthesized mesostructured silicas

**Table 2.** Characterization data for mesostructured silicas

<b>Silica</b>	<b>Channel structure</b>	<b>Particle morphology (size, <math>\mu\text{m}</math>)</b>	<b><math>L_0^a</math> (<math>\text{mmol g}^{-1}</math>)</b>	<b><math>S_{\text{BET}}^b</math> (<math>\text{m}^2 \text{g}^{-1}</math>)</b>	<b>BJH<sup>c</sup> pore diameter (<math>\text{\AA}</math>)</b>	<b>Pore volume (<math>\text{cm}^3 \text{g}^{-1}</math>)</b>
Ethane-PMO	3 D Wormhole-like	Spherical (2.5)	-	958	35	0.57
Ethane-PMO-C18	3 D Wormhole-like	Spherical (2.5)	0.24	677	26	0.42
MSU-2	3 D Wormhole-like	Spherical (1.0)	-	852	34	0.77
MSU-2-C18	3 D Wormhole-like	Spherical (1.0)	0.26	682	29	0.62
HMS	3 D Wormhole-like	Spherical (1.7)	-	962	26	0.88
HMS-C18	3 D Wormhole-like	Spherical (1.7)	0.23	889	23	0.71
SBA-15	1D hexagonal parallel channels	Rod-like (1 x 0.4)	-	764	65	0.74
SBA-15-C18	1D hexagonal parallel channels	Rod-like (1 x 0.4)	0.23	685	64	0.69
MCM-41	1D hexagonal parallel channels	Rod-like (1.5 x 0.2)	-	1101	30	1.03
MCM-41-C18	1D hexagonal parallel channels	Rod-like (1.5 x 0.2)	0.42	898	23	0.76

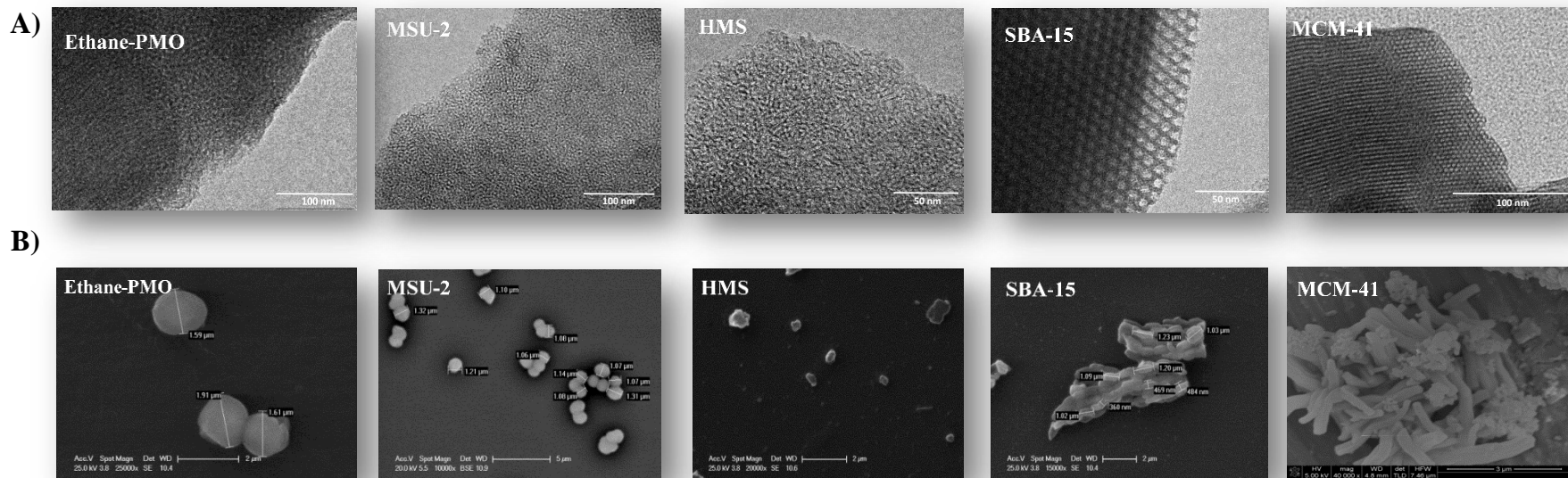
<sup>a</sup> $L_0$  = mmol of C18 per gram of functionalized mesoporous silica

<sup>b</sup> $S_{\text{BET}}$  = Specific surface area calculated by Brunauer-Emmett-Teller (BET) method

<sup>c</sup>BJH = Pore size distribution calculated by Barret-Joyner-Halenda (BJH) method

TEM micrographs (Fig. 2A) confirmed the disordered structure of HMS, MSU-2 and ethane-PMO, showing irregularly aligned mesopores with relatively uniform pore sizes (wormhole-like pore arrangement). Conversely, SBA-15 and MCM-41 demonstrated clear arrangement of ordered hexagonal pores with uniform size. SEM pictures (Fig. 2B) showed the spherical morphology of MSU-2, HMS and ethane-PMO, with mean diameters around 1, 1.7 and 2.5  $\mu\text{m}$ , respectively. Alternatively, the particle morphology was rod-like for SBA-15 (1 x 0.4  $\mu\text{m}$ ) and MCM-41 (1.5 x 0.2  $\mu\text{m}$ ). After functionalization, all materials kept their morphology, particle size and structure.

Elemental analysis confirmed that C18 groups were successfully grafted in each material, and C18 density ( $L_0$ ) was higher with the increase of surface area (Table 2), which was also confirmed by TGA (Fig. 3).



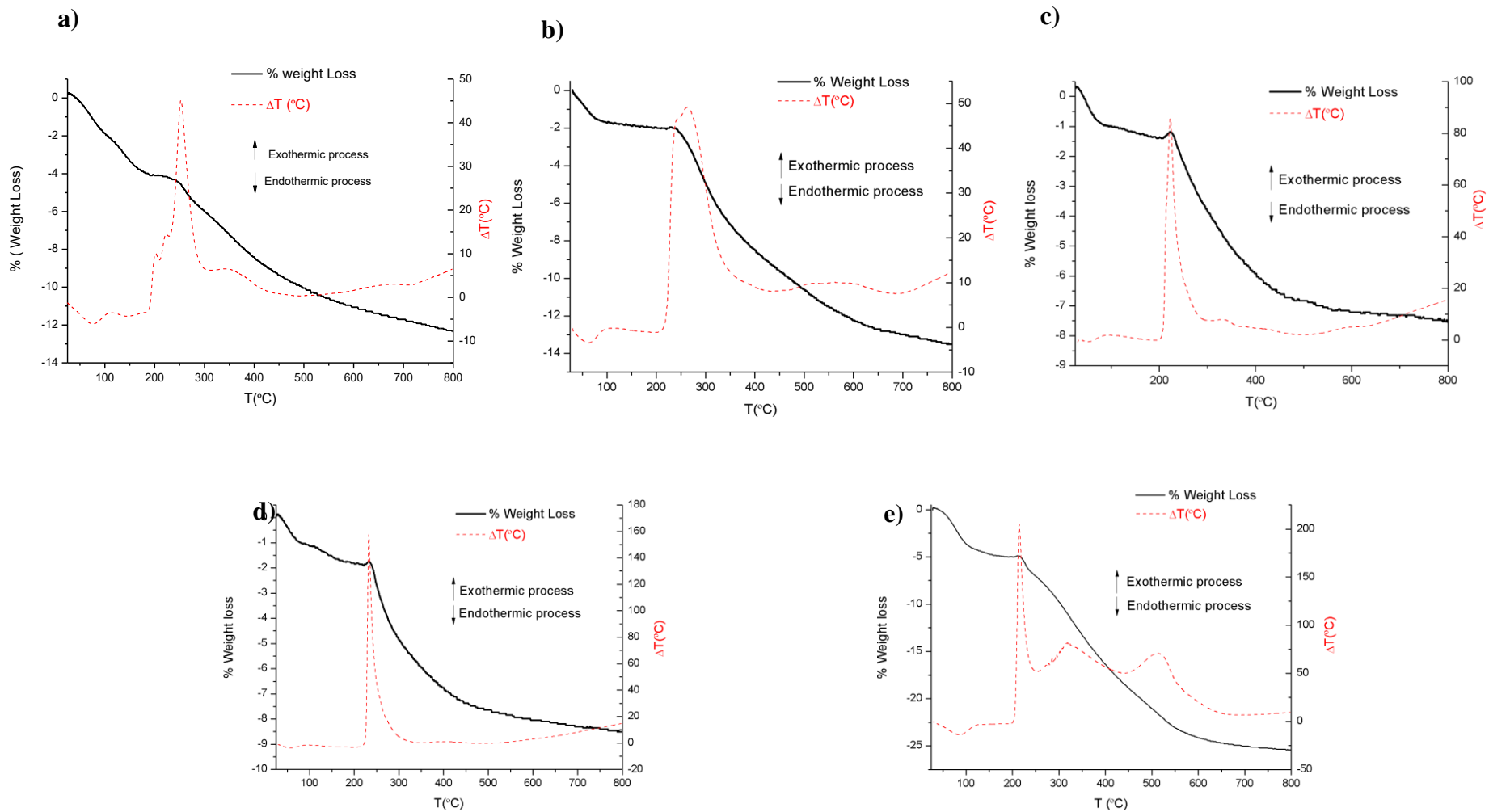


**Fig. 3** TGA curves of the C18 modified mesoporous silicas: SBA-15-C18 (a), MCM-41-C18 (b), HMS-C18 (c), MSU-2-C18 (d) and ethane-PMO-C18 (e).

### 3.2. Method performance with wormhole-like mesostructured silicas

Ethane-PMO was tested as sorbent, since it has ethylene (-CH<sub>2</sub>CH<sub>2</sub>-) bridges in its internal structure where analytes can interact, however, results were unsatisfactory (Fig. 4). Conversely, ethane-PMO-C18 was clearly more effective than non-modified ethane-PMO (Fig. 4). Therefore, post-functionalization with C18 improved the extraction of analytes because of the hydrophobic interactions between analytes and C18 chains, which particularly enhanced retention of the less polar compounds. Nevertheless, ethane-PMO-C18 was not effective (recovery <50%) for  $\beta$ -agonists, most of the  $\beta$ -blockers and some NSAIDs (tolfenamic acid and vedaprofen). MSU-2-C18 provided good recoveries for most target analytes, nevertheless, best results were achieved with HMS-C18, since better adsorption was observed for specific analytes such as, cimaterol, terbutaline, atenolol, ractopamine, clenproperol, carprofen, ibuprofen and tolfenamic acid (Fig. 4). Additionally, relative standard deviation (RSD) values (n=6) were, generally, lower in comparison with MSU-2-C18. This fact was attributed to the bigger mean diameter of HMS-C18 (near 2  $\mu$ m), which favours cartridge packaging and helps to reduce pressure drop of the device, achieving higher reproducibility in the SPE procedure. The bad results of ethane-PMO-C18 in comparison with MSU-2-18 and HMS-C18 could be due to a worse accessibility and availability of the C18 groups attached on the silica because of the presence of internal ethylene (-CH<sub>2</sub>CH<sub>2</sub>-) bridges in its structure. Therefore, based on these data, HMS-C18 showed the highest potential as SPE sorbent for multi-residue extraction of the target analytes from meat samples.

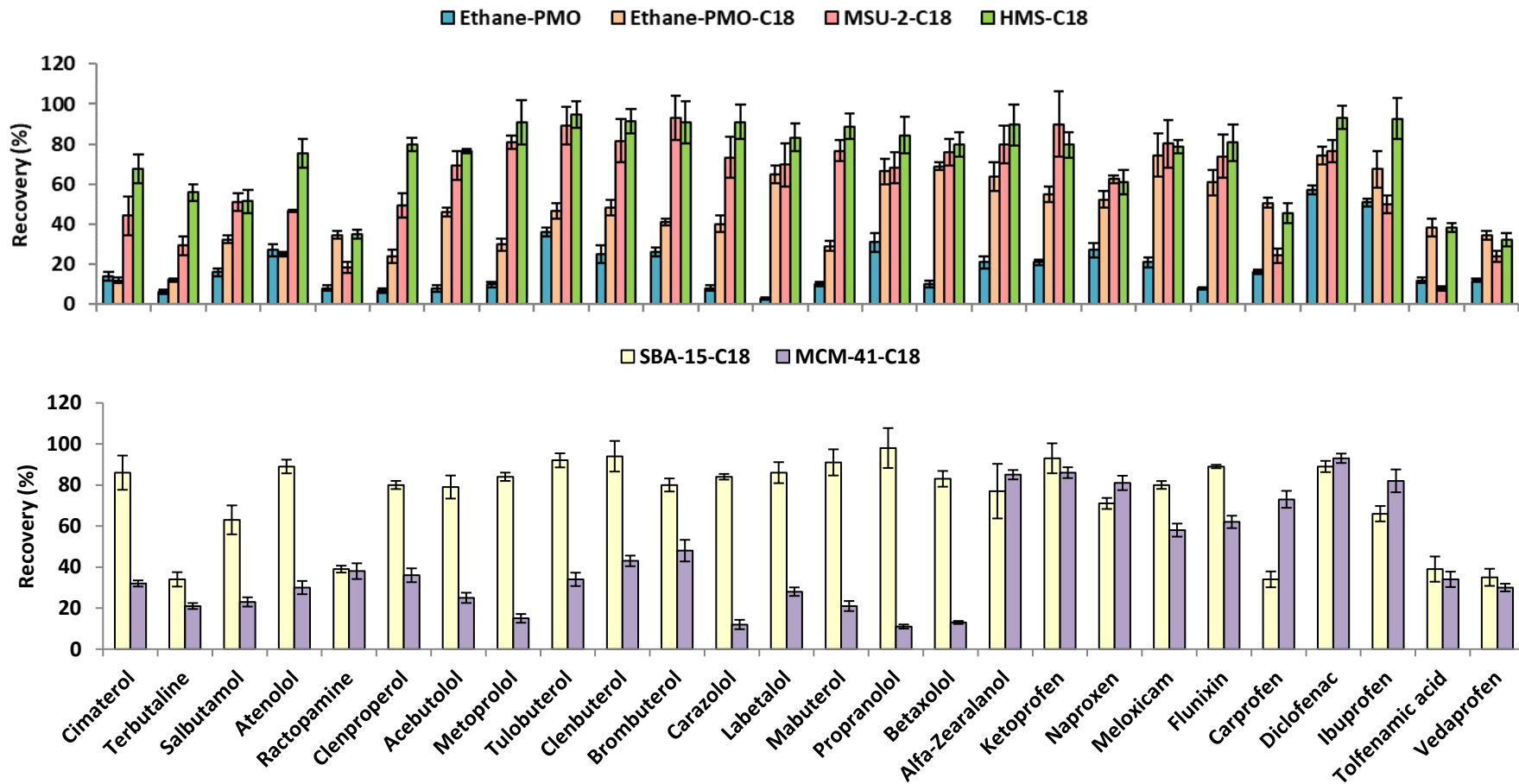


**Fig. 4** Recovery percentages obtained from the analysis of spiked meat samples extracted with SPE cartridges packed with 100 mg of mesostructured silicas. Error bars represent standard deviation of sample replicates (n=6).

### 3.3. Comparison of HMS-C18 with hexagonal ordered mesoporous silicas

Despite having high surface area (Table 2), MCM-41-C18 was not successful for extraction of  $\beta$ -blockers and  $\beta$ -agonists (recoveries between 11 - 48%) (Fig. 4). However, good recoveries were achieved for  $\alpha$ -zearalanol (85%) and NSAIDs (58 - 93%, except tolfenamic acid and vedaprofen). These results could be due to the high amount of C18 groups attached on the silica, since MCM-41-C18 was the material with the highest L0 (Table 2), providing more hydrophobic interactions which enhance retention of less polar compounds. Nevertheless, the high L0 of MCM-41-C18 may lead to a lesser amount of residual non-modified silanol groups on the silica, providing less polar secondary interactions (by hydrogen bonding interactions) and, consequently, reducing retention of the most polar compounds. Moreover, the 1D hexagonal parallel channels of this material, with small pore diameter (23 Å), and the rod-like particle morphology (1.5 x 0.2  $\mu\text{m}$ ) lead to a poor mass transfer inside the mesopores. Conversely, SBA-15-C18 was clearly more effective, since recoveries were, generally, higher for all compounds (Fig. 4). These results could be attributed to the fact that SBA-15-C18 contains accessible functional groups (64 Å of pore diameter), which are homogeneously distributed in the material, compared to MCM-41-C18. Thus, in SBA-15-C18 analytes may experience a reversed-phase sorption with the C18 groups by hydrophobic interactions and polar secondary interactions by hydrogen bonding interactions, due to the high number of residual non-modified silanol groups in the material. Regarding HMS-C18, despite having different structure, it exhibited similar behaviour to SBA-15-C18 (Fig. 4). Generally, good recoveries values were obtained with both materials, however, significant improvements were observed in the retention of terbutaline, carprofen and ibuprofen using HMS-C18 (Fig. 4). Additionally, HMS presents some advantages over SBA-15 related to its synthesis and morphology, since the template route used in its synthesis produces mesostructures with thicker pore walls, which improve thermal and hydrothermal stability of the mesopore framework, and where a substantial fraction of  $(\text{SiO})_3\text{Si-OH}$  groups are incorporated, instead of being located exclusively at surface channels [9]. Additionally, the neutral and extensively cross-linked character of HMS frameworks allows the efficient and environmentally benign recovery of the cost-intensive template by simple solvent extraction. Furthermore, small particle sizes of HMS with spherical morphology provide better access to the wormlike-framework-confined mesopores in extraction processes, as well as a more homogeneous packaging of SPE cartridges, which helps to achieve regular flow and good extraction efficiency. Therefore, HMS-C18 could be consider a promising SPE sorbent for multi-residue extraction of contaminants from different nature and polarity, and an alternative to classical commercial sorbents, such as amorphous silica, or other ordered mesoporous silicas, such as SBA-15 and MCM-41.



#### **4. Conclusions**

HMS-C18 is a promising sorbent for multi-residue extraction of contaminants from food matrices, providing good performance due to its spherical morphology and its wormhole-like structure, moreover, functionalization with C18 increases its versatility to extract compounds from different nature and polarity thanks to its hydrophilic-lipophilic balance. Additionally, its synthesis presents some advantages over other mesostructured silicas, since it is more cost-effective and environmentally friendly.

#### **Acknowledgments**

Authors thank financial support from the Comunidad of Madrid and European funding from FEDER program (Project S2013/ABI-3028, AVANSECAL).

## References

- [1] C. Robert, N. Gillard, P.Y. Brasseur, G. Pierret, N. Ralet, M. Dubois, P. Delahaut, Rapid multi-residue and multi-class qualitative screening for veterinary drugs in foods of animal origin by UHPLC–MS/MS, *Food Addit. Contam. A* 30 (2013) 443–457.
- [2] A. Azzouz, B. Souhail, E. Ballesteros, Determination of residual pharmaceuticals in edible animal tissues by continuous solid-phase extraction and gas chromatography–mass spectrometry, *Talanta* 84 (2011) 820–828.
- [3] N. Casado, D. Pérez-Quintanilla, S. Morante-Zarcelo, I. Sierra, Current development and applications of ordered mesoporous silicas and other sol-gel silica-based materials in food sample preparation for xenobiotics analysis, *TrAC*. 88 (2017) 167-184.
- [4] D. Pérez-Quintanilla, A. Sánchez, I. del Hierro, M. Fajardo, I. Sierra, Solid phase extraction of Pb(II) in water samples using a new hybrid inorganic-organic mesoporous silica prior to its determination by FAAS, *Microchim. Acta* 165 (2009) 291-298.
- [5] D. Pérez-Quintanilla, A. Sánchez, I. del Hierro, M. Fajardo, I. Sierra, Synthesis and characterization of novel mesoporous silicas of the MSU-X family for environmental applications, *J. Nanosci. Nanotechnol.* 9 (2009) 4901-4909.
- [6] G. Zhu, H. Zhong, Q. Yang, C. Li, Chiral mesoporous organosilica spheres: synthesis and chiral separation capacity, *Micropor. Mesopor. Mater.* 116 (2008) 36-43.
- [7] D. Zhao, Q. Huo, J. Feng, B.F. Chmelka, G.D. Stucky, Nonionic Triblock and Star Diblock Copolymer and Oligomeric Surfactant Syntheses of Highly Ordered, Hydrothermally Stable, Mesoporous Silica Structures, *J. Am. Chem. Soc.* 120 (1998) 6024-6036.
- [8] M.V. Landau, S.P. Varkey, M. Herskowitz, O. Regev, S. Pevzner, T. Sen, Z. Luz, Wetting stability of Si-MCM-41 mesoporous material in neutral, acidic and basic aqueous solutions, *Micropor. Mesopor. Mater.* 33 (1999) 149-163.
- [9] W. Zhang, T. Pauly, T. Pinnavaia, Tailoring the framework and textural mesopores of HMS molecular sieves through and electrically neutral ( $S^{0I^0}$ ) assembly pathway, *Chem. Mater.* 9 (1997) 2491-2498.